Science Advances
AAAS

Supplementary Materials for

Modeling embryo-endometrial interface recapitulating human embryo implantation

Shun Shibata *et al.*

Corresponding author: Shun Shibata, shun.shibata.a3@tohoku.ac.jp; Takahiro Arima, tarima@med.tohoku.ac.jp

Sci. Adv. **10**, eadi4819 (2024)
DOI: 10.1126/sciadv.adi4819

The PDF file includes:

Figs. S1 to S9
Table S1
Legends for data S1 to S3

Other Supplementary Material for this manuscript includes the following:

Data S1 to S3

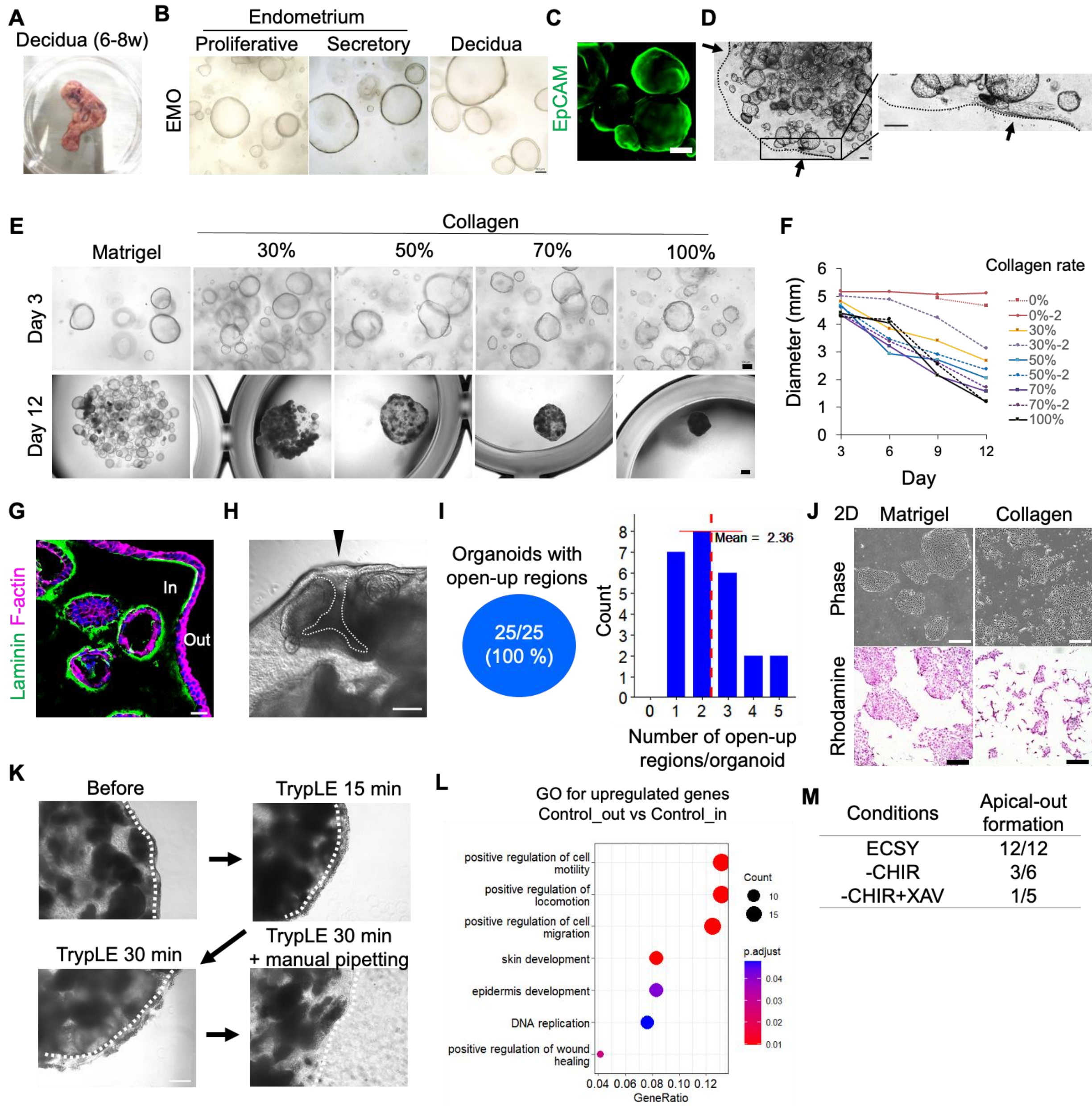

Fig. S1. Generation of apical-out endometrial organoids (AO-EMO). (**A**) Human decidua (6–9 weeks gestation). (**B**) Bright-field images of human endometrium- and decidua-derived EMO. Scale bar, 100 µm. (**C**) Whole-mount imaging of EMO stained for EpCAM. Scale bar, 500 µm. (**D**) Phase contrast images of EMO cultured in a collagen-based culture on day 3. Black arrows indicate areas where epithelial cells began to cover the surface and the collagen-based gel started to contract. Dashed lines outline the outer edge of the gel. Scale bars, 200 µm. (**E**) Bright-field images of EMO in Matrigel and 30%, 50%, 70%, and 100% collagen-based gels on days 3 and 12 of culture. Scale bars, 100 µm (upper) and 500 µm (lower). (**F**) Quantification of diameters of EMO or gel. (**G**) Immunostaining image of AO-EMO stained for laminin (green) and F-actin (magenta); nuclei are stained with Hoechst (blue). Scale bar, 20 µm. (**H**) Phase contrast image of the open-up region in AO-EMO. The black arrowhead indicates the open-up region. The dotted

line traces the outline of the inside of the endometrial epithelium. Scale bar, 100 µm. (**I**) Quantification of organoids that possess open-up regions (left) and the number and distribution of open-up regions per organoid. The vertical red dashed line indicates the mean value, while the horizontal red lines represent the standard deviation. (**J**) Phase contrast and rhodamine staining images of 2D-cultured human EMO on Matrigel- or collagen-coated dishes. Scale bars, 500 µm (upper) and 200 µm (lower). (**K**) Phase contrast images of AO-EMO during the separation process. Scale bar, 200 µm. (**L**) GO terms related to biological processes enriched in outer (Control_out) versus inner (Control_in) cells of AO-EMO pre-treated with hormone. (**M**) Quantification of AO formation rate under various culture conditions.

A

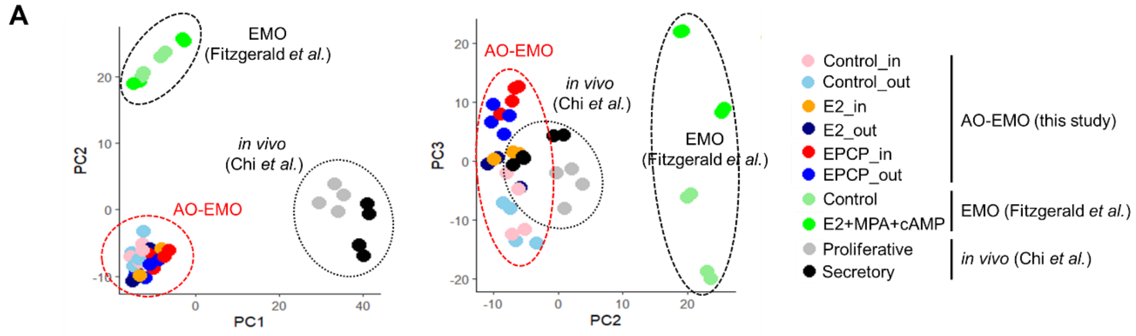

B

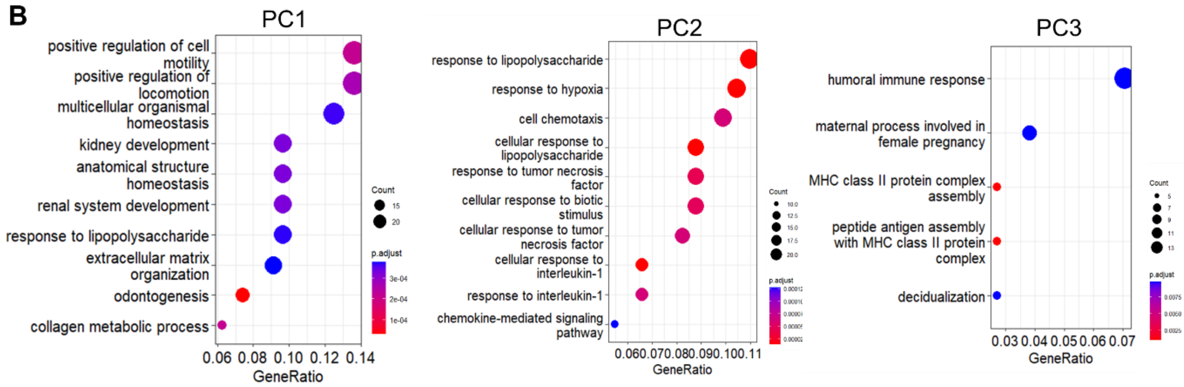

C

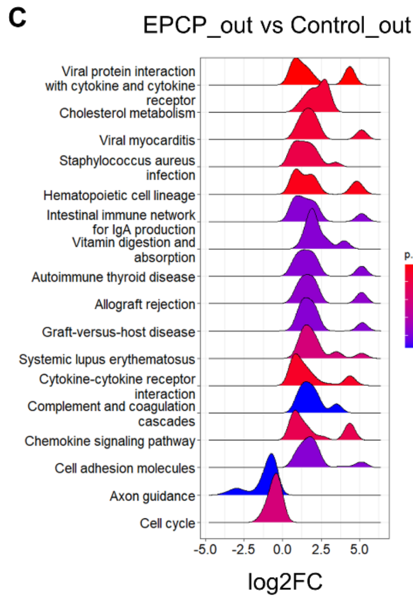

D

ERA genes_UP (143 genes) FC > 3

Category	Term	Count	PValue
KEGG_PATHWAY	Complement and coagulation cascades	7	1.57E-04
KEGG_PATHWAY	Mineral absorption	5	0.001772

E

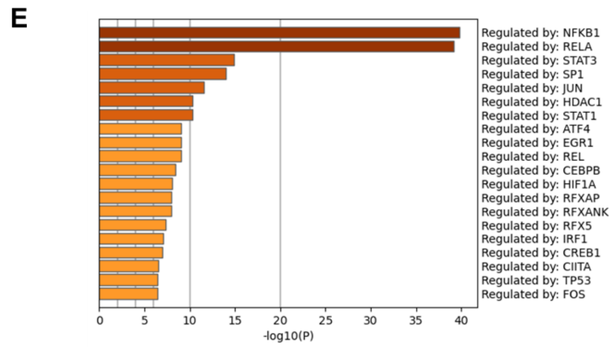

F

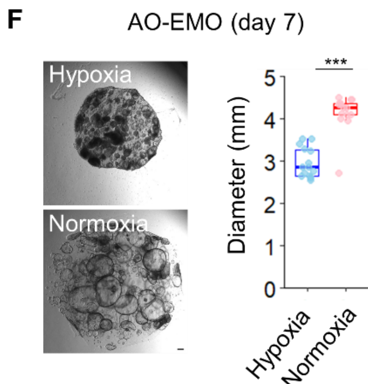

G

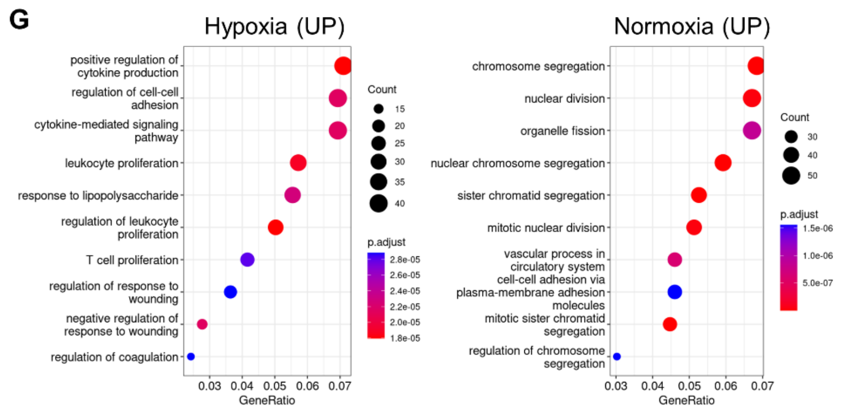

Fig. S2. Collagen-based culture enhances the maturation and spatial heterogeneity of endometrial epithelial cells.

(**A**) Principal component analysis of the transcriptome of AO-EMO, conventional EMO (*31*), and *in vivo* endometrial epithelial cells (*33*). (**B**) GO terms (biological processes) enriched in genes of PC1, PC2, and PC3. (**C**) Pre-ranked gene set enrichment analysis (GSEA) of upregulated genes in outer cells treated with hormone (EPCP_out) versus control (Control_out). (**D**) KEGG enrichment analysis of extracted upregulated genes (143 genes) in the listed Endometrial Receptivity Analysis (ERA) test (*36*). (**E**) Predicted upstream transcription factors using upregulated genes in EMO cultured in collagen. (**F**) Bright-field images (left) and diameters (right) of AO-EMO cultured under hypoxic and normoxic conditions on day 7 of culture. Scale bar, 200 µm. n = 15 AO-EMO. (**G**) GO terms related to biological processes enriched in upregulated genes in AO-EMO cultured under hypoxic (left) and normoxic (right) conditions.

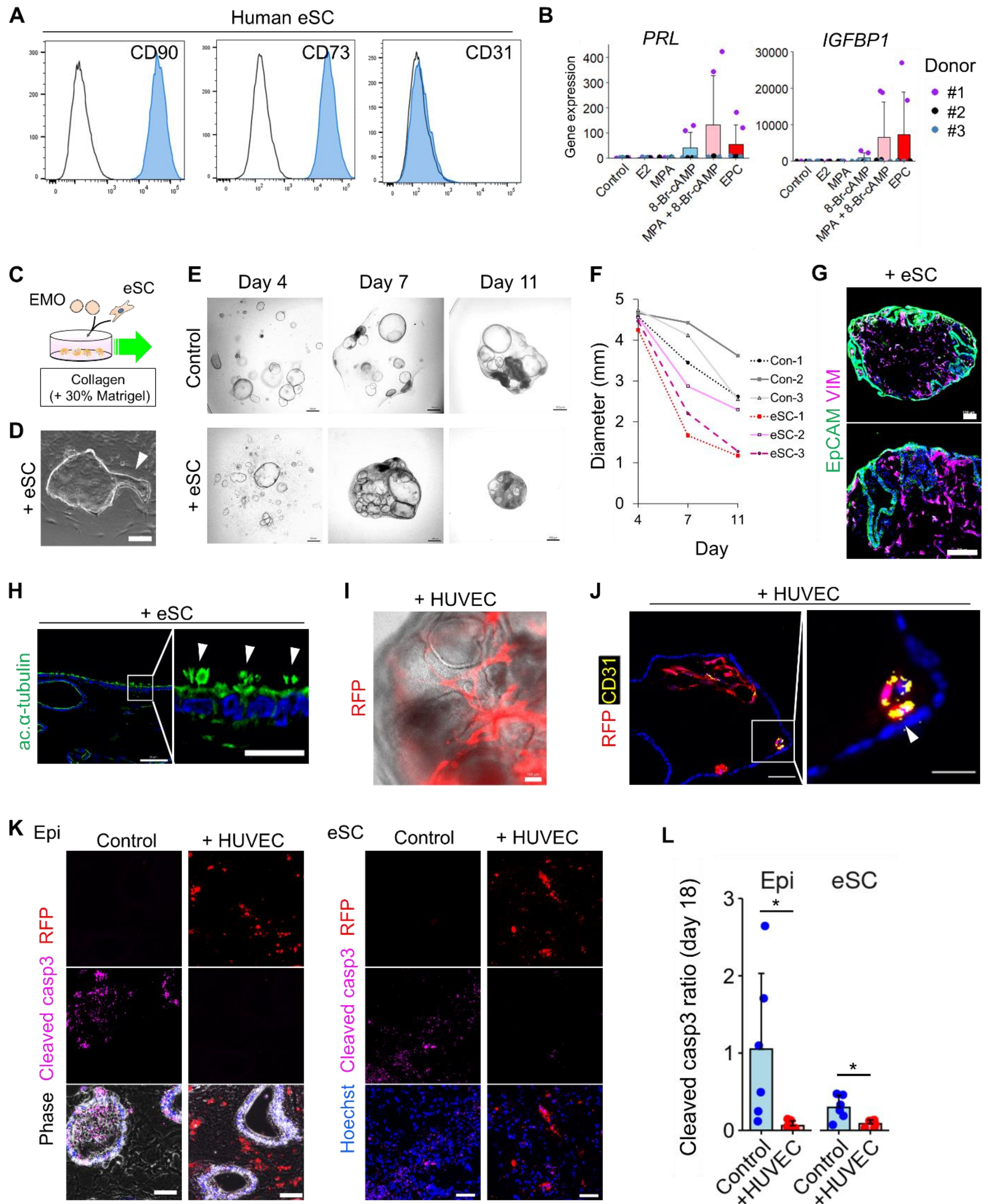

Fig. S3. Integrating stromal cells and vascular network into AO-EMO. (**A**) Flowcytometric analysis of human eSC with endometrial stromal (CD90 and CD73) and endothelial (CD31) markers. (**B**) Gene expression levels of eSC treated with vehicles (Control), E2, MPA, 8-Br-cAMP, MPA + 8-Br-cAMP, and E2 + MPA + 8-Br-cAMP (EPC). Data shown as mean ± SD; n

= 6 from three individual donors. (**C**) Schematic representation of the culture method. (**D**) Phase contrast image of EMO co-cultured with eSC. The arrowhead indicates the protrusion of EMO. Scale bar, 100 µm. (**E**) Bright-field images of EMO co-cultured with or without eSC in collagen-based gel on days 4, 7, and 11. Scale bars, 500 µm. (**F**) Quantification of diameters of EMO or gel of AO-EMO with or without eSC. (**G**) Fluorescence images of AO-EMO including eSC stained for EpCAM and VIM; nuclei stained with Hoechst (blue). Scale bars, 100 µm. (**H**) Fluorescence images of AO-EMO including eSC stained for acetylated (ac.) α-tubulin; nuclei are stained with Hoechst (blue). Scale bars, 50 µm (upper) and 20 µm (lower). Arrowheads indicate ac. α-tubulin^{+} cilia. (**H**) Bright-field and fluorescence image of AO-EMO, including RFP-HUVEC. Scale bar, 500 µm. (**I**) Bright-field and fluorescence image of AO-EMO, including eSC and RFP-HUVEC. Scale bar, 500 µm. (**J**) Fluorescence images of AO-EMO including RFP-HUVEC stained for CD31; nuclei stained with Hoechst (blue). Arrowheads indicate luminal structures. Scale bars, 50 µm and 20 µm (magnified). (**K**) Phase contrast and fluorescence images of AO-EMO co-cultured with RFP-HUVEC (red) and AO-EMO + eSC co-cultured with RFP-HUVEC (red), cultured for 18 days stained for cleaved caspase (Casp)-3; nuclei stained with Hoechst (blue). Scale bars, 50 µm. (**L**) Quantification of cleaved Casp3^{+} ratio normalized to nuclei. Data shown as mean ± SD; $^{*}P < 0.05$; n = 6 frozen sections from three independent experiments.

A

AO-EMO + eSC/HUVEC

Control

Hormone

Nuclei isolation

Sorting

snRNA-seq

DAPI

FSC

Phase DAPI

20 µm

B

LGR5 GUCY1A2 SOX9

MKI67 CD34 PAEP

PIFO WNT7A PAX2

C

NH Secretory WNT7A+ Stromal LGR5+ PV-like PAX2+ Proliferative Ciliated

D

Luminal

Glandular

SOX9+ (#10, #13)

Lymphocytes

Secretory

Ciliated

E2-induced

Endothelial

No hormone (NH)

Pre-ciliated

Stromal fibroblasts

eS

PV

AO-EMO + eSC/HUVEC

in vivo (Wang *et al.*)

in vivo (Garcia *et al.*)

EMO (Garcia *et al.*)

UMAP_2

UMAP_1

E

AO-EMO + eSC/HUVEC

EMO (Garcia *et al.*)

in vivo (Garcia *et al.*)

in vivo (Wang *et al.*)

F

AO-EMO + eSC/HUVEC

EMO (Garcia *et al.*)

Ciliated

SOX9+

Stroma

Endothelial

Proliferative

UMAP_2

UMAP_1

G

anion transmembrane transporter activity

organic anion transmembrane transporter activity

carboxylic acid transmembrane transporter activity

organic acid transmembrane transporter activity

sodium-independent organic anion transmembrane transporter activity

manganese ion transmembrane transporter activity

cadherin binding

actin binding

actin filament binding

cell-cell adhesion mediator activity

integrin binding

extracellular matrix structural constituent

extracellular matrix structural constituent conferring tensile strength

platelet-derived growth factor binding

collagen binding

GTPase activator activity

GTPase regulator activity

nucleoside-triphosphatase regulator activity

proteoglycan binding

carbohydrate kinase activity

catalytic activity, acting on DNA

tubulin binding

microtubule binding

ATP-dependent activity, acting on DNA

single-stranded DNA binding

microtubule motor activity

cytoskeletal motor activity

minus-end-directed microtubule motor activity

nucleoside diphosphate kinase activity

protein folding chaperone

unfolded protein binding

ATP-dependent protein folding chaperone

heat shock protein binding

ubiquitin protein ligase binding

MHC class II protein complex binding

guanyl-nucleotide exchange factor activity

SH3 domain binding

phosphoric ester hydrolase activity

NH (170) Secretory (154) WNT7A+ (174) Stromal (170) PV-like (176) PAX2+ (172) Proliferative (183) Ciliated (143) SOX9 #10 (165) Endo (172) SOX9+ #13 (185)

GeneRatio

p.adjust

H

Hormone (EPCP) - UP

ameboidal-type cell migration

epithelial cell migration

epithelium migration

endodermal cell differentiation

renal system development

tissue migration

formation of primary germ layer

urogenital system development

qscore

Hormone (EPCP) - DOWN

epithelial cilium movement involved in extracellular fluid movement

extracellular transport

motile cilium assembly

cilium organization

synapse organization

vascular transport

transport across blood-brain barrier

cilium assembly

qscore

I

Control

Hormone

PGR PCNA IL15

Stromal Stromal Stromal

FOXO1 S100A4 LMCD1

Stromal Stromal Stromal

Expression level

Fig. S4. Characterization of AO-EMO at the single-cell level. (**A**) Schematic representation of the experimental procedure (upper). Flow cytometry image for DAPI$^+$ sorting of AO-EMO + eSC/HUVEC, and phase contrast and fluorescence images of sorted nuclei (lower); Scale bar, 20 μm. (**B**) Feature plots showing expression levels and distribution of marker genes. (**C**) Heatmap showing the top five most upregulated genes in each cluster of AO-EMO + eSC/HUVEC. (**D and E**) UMAP projection of the four datasets integration (*30, 35*). The pie charts show the proportion of each cell type occupied by each dataset (D). Each of the four datasets is overlaid with a unique color on the integrated data (E). (**F**) UMAP plot representing the integrated data from AO-EMO + eSC/HUVEC and EMO (Garcia *et al.*). (**G**) Dot plot showing enriched GO terms in each cluster of AO-EMO + eSC/HUVEC. (**H**) Bar graph representing GO term (BP) enriched in AO-EMO + eSC/HUVEC with (upper) or without (lower) hormone (EPCP) treatment. (**I**) Violin plots representing the expression levels of hormone-responsive genes of the stromal population in AO-EMO + eSC/HUVEC with or without hormone treatment.

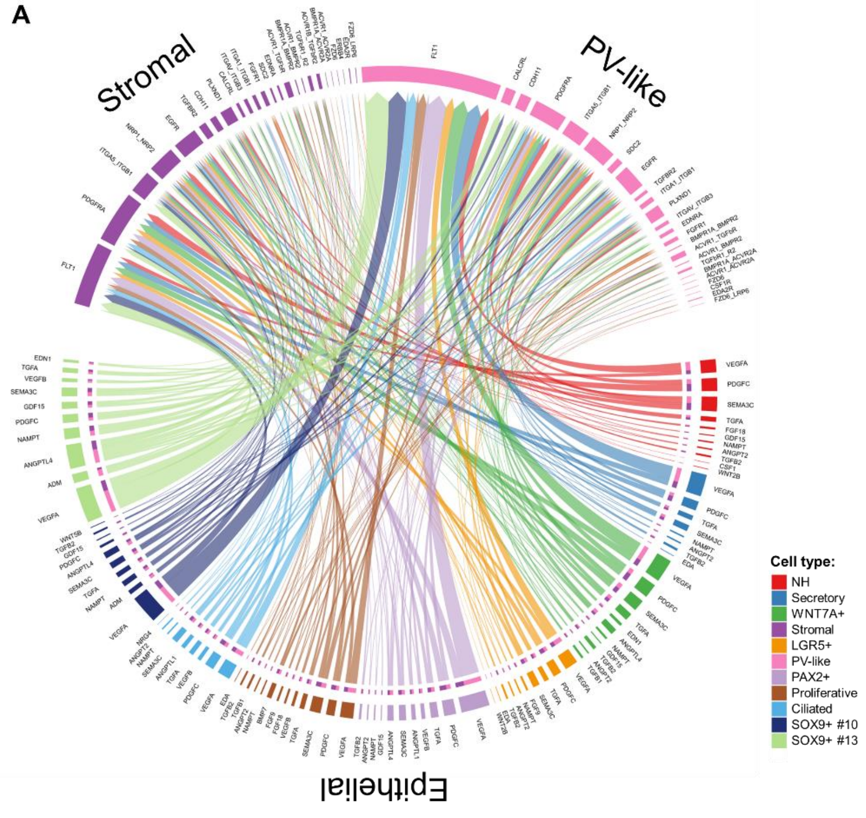
A
Stromal
PV-like
Epithelial
Cell type:
NH
Secretory
WNT7A+
Stromal
LGR5+
PV-like
PAX2+
Proliferative
Ciliated
SOX9+ #10
SOX9+ #13

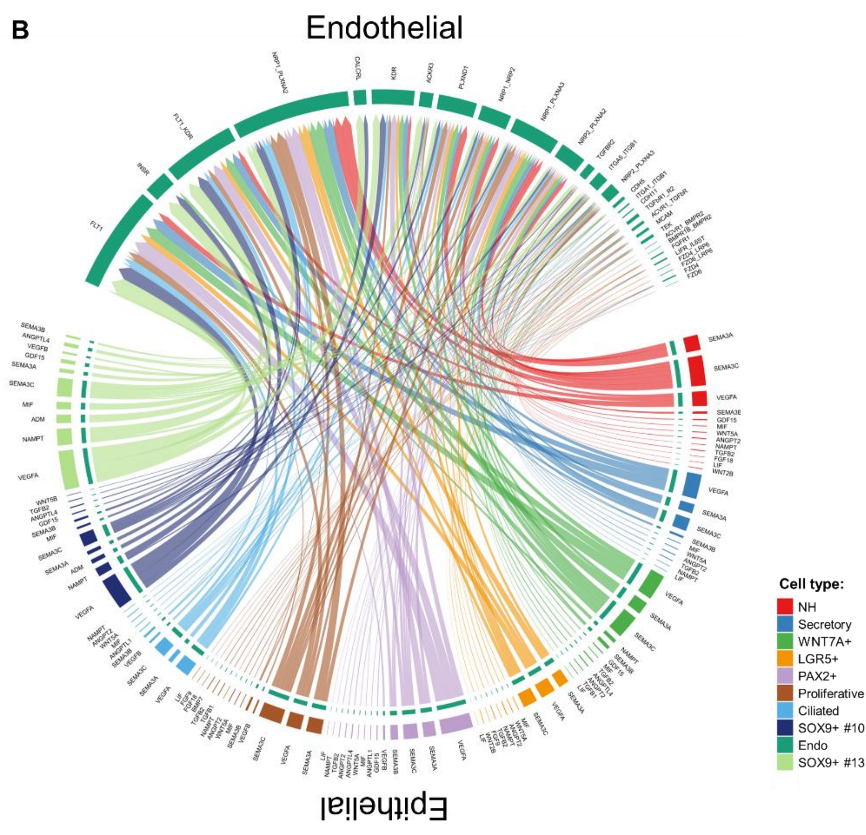
B
Endothelial
Epithelial
Cell type:
NH
Secretory
WNT7A+
LGR5+
PAX2+
Proliferative
Ciliated
SOX9+ #10
Endo
SOX9+ #13

Fig. S5. Ligand-receptor analysis in AO-EMO + eSC/HUVEC snRNA-seq data. This visualization represents inferred cellular communication patterns between different cell types based on ligand-receptor interactions. (**A**) Potential interactions between epithelial and endothelial cells, while (**B**) highlights those between epithelial and stromal cells.

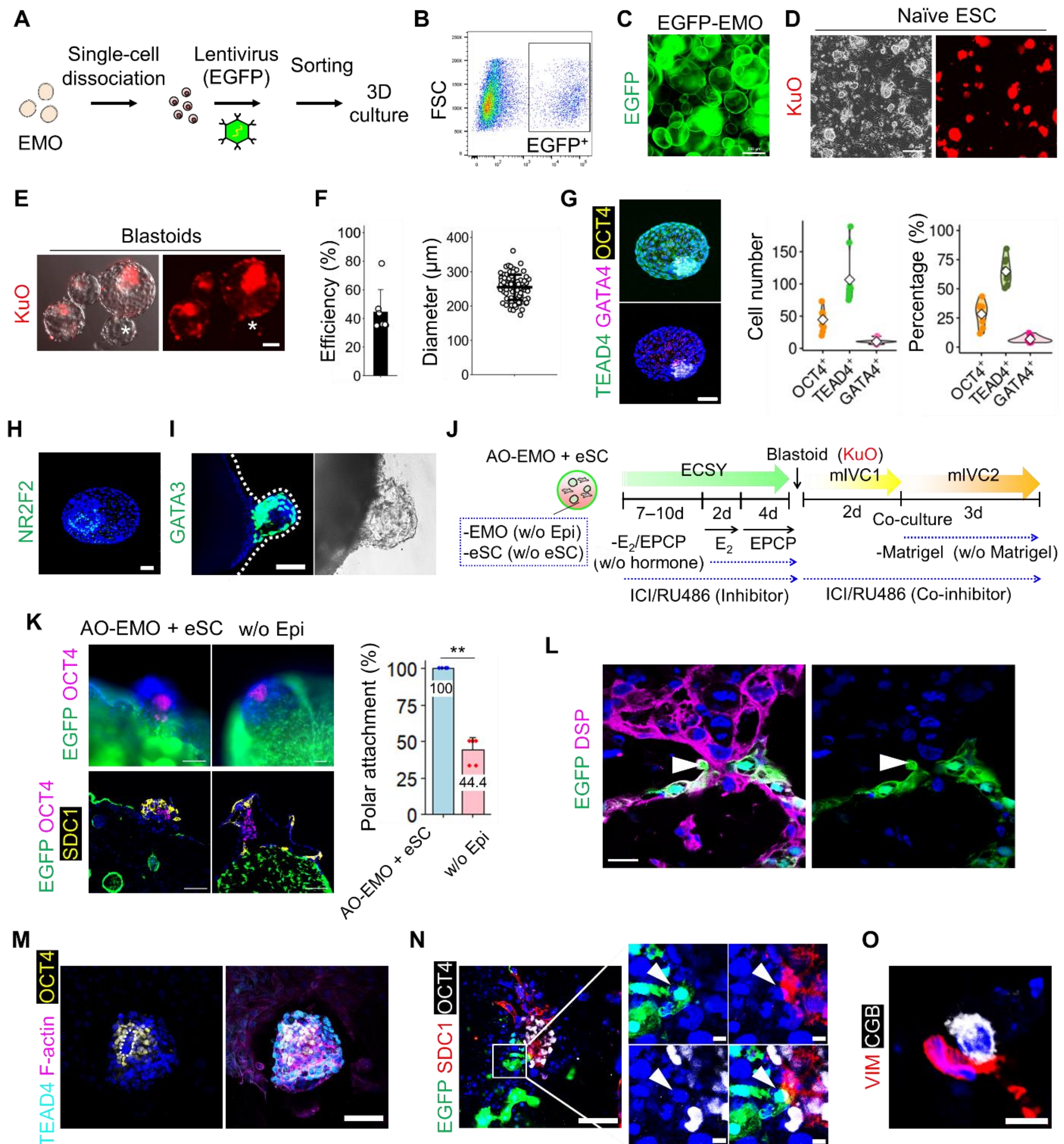

Fig. S6. Feto–maternal assembloids mimic human embryo implantation. (**A**) Schematic representation of the experimental procedure for generating EGFP-expressing human EMO (EGFP-EMO). (**B**) Flow cytometry graph for EGFP⁺ sorting of lentivirus-infected EMO. (**C**) Fluorescence image of EGFP-EMO. Scale bar, 500 μm. (**D**) Phase contrast and fluorescence (KuO: red) images of naïve human ESC. Scale bar, 200 μm. (**E**) Bright-field and fluorescence images of KuO⁺ human blastoids. Scale bar, 100 μm. * indicates blastoid lacking ICM-like cells. (**F**) Quantification of formation efficiency (left) and diameter (right) of blastoids. n = 6 independent induction experiments (left) and 85 blastoids (right). (**G**) Whole-mount imaging of human blastoid stained for TEAD4, GATA4, and OCT4 (left). Scale bar, 100 μm. Quantification

of the $OCT4^+$, $TEAD4^+$, and $GATA4^+$ cells, and their respective proportions of the total cell number in blastoids (right). n = 9 blastoids. (**H**) Whole-mount imaging of human blastoid stained for NR2F2; nuclei stained with Hoechst (blue). Scale bar, 100 μm. (**I**) Bright-field and whole-mount imaging of attached blastoid stained for GATA3; nuclei stained with Hoechst (blue). Scale bar, 100 μm. (**J**) Schematic representation of the experimental procedure for quantifying the adhesion rate of blastoids in various culture conditions. (**K**) Whole-mount imaging (upper) and fluorescence images of frozen sections (lower) of feto–maternal assembloid (Epi, $EGFP^+$ [AO-EMO + eSC]; eSC, $EGFP^+$ [w/o Epi]) stained for OCT4 and SDC1; nuclei stained with Hoechst (blue). Scale bars, 100 μm (left). Quantification of the ratio of polar attachment of blastoids (right). n = 7 (AO-EMO + eSC) and 6 (w/o Epi) independent co-culture experiments. $^{**}P < 0.01$. (**L**) Fluorescence images of feto–maternal assembloid stained for Desmoplakin (DSP); nuclei stained with Hoechst (blue). Scale bar, 20 μm. Arrowheads indicate invading blastoids. (**M** and **N**) Whole-mount imaging of feto–maternal assembloid (Epi: $EGFP^+$) stained for OCT4 and TEAD4 (M) or SDC1 (N); nuclei stained with Hoechst (blue). Arrowheads indicate $EGFP^+/SDC1^+$ cells. Scale bars, 100 μm and 10 μm (magnified). (**O**) Fluorescence images of feto–maternal assembloid stained for VIM and CGB; nuclei stained with Hoechst (blue). Scale bar, 10 μm.

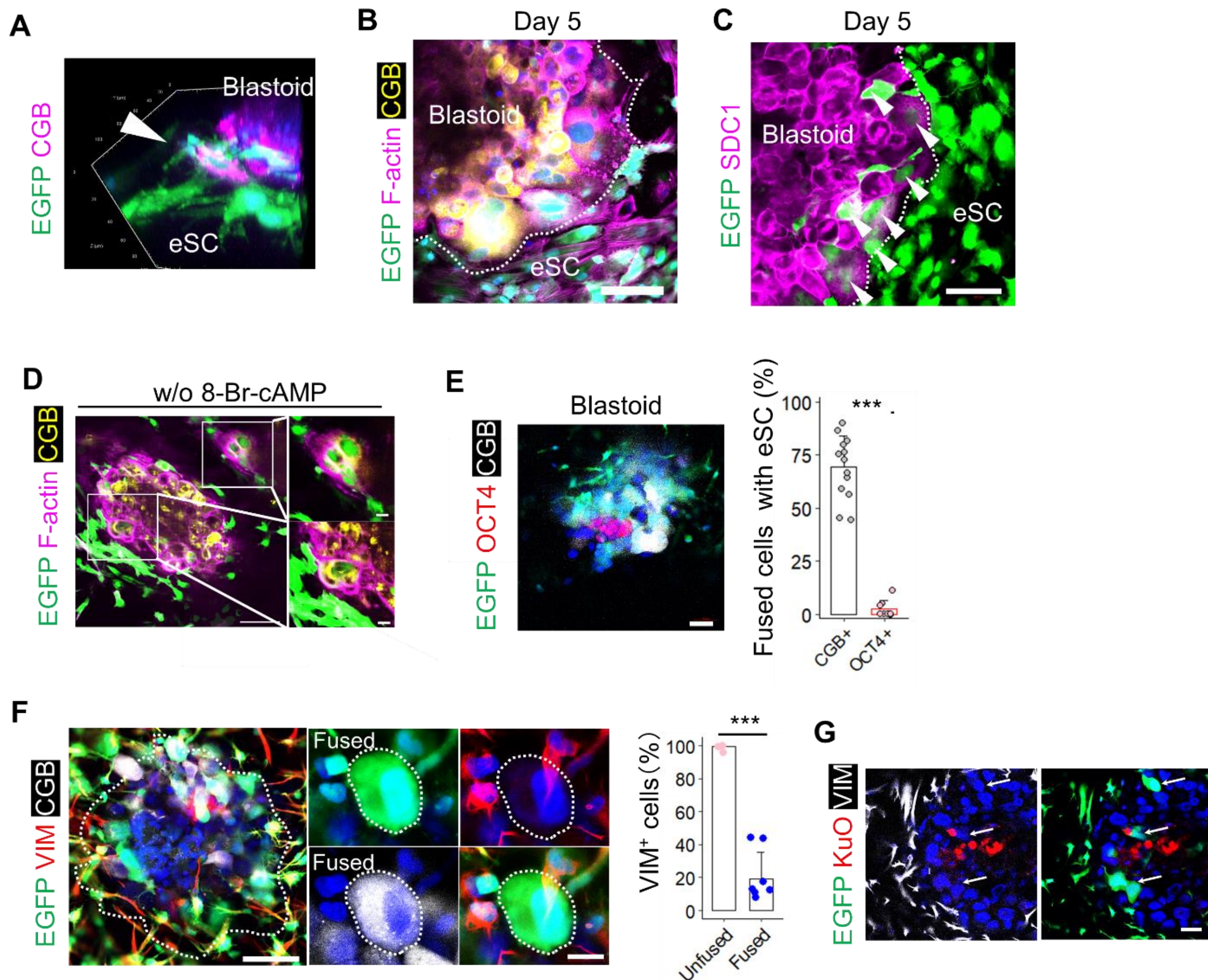

Fig. S7. The invading syncytium fuses with endometrial stromal cells. (**A**) Reconstructed 3D image of EGFP$^+$/CGB$^+$ cells at the blastoid–eSC interface. (**B**) Whole-mount imaging of blastoids co-cultured with eSC (EGFP$^+$) on day 5 stained for CGB and F-actin; nuclei stained with Hoechst (blue). Scale bar, 100 µm. (**C**) Whole-mount imaging of blastoids co-cultured with eSC (EGFP$^+$) on day 5 stained for SDC1; nuclei stained with Hoechst (blue). Scale bar, 100 µm. Arrowheads point to EGFP$^+$ nuclei within SDC1$^+$ cells. The dashed line delineates the interface between the blastoid and eSC regions. (**D**) Whole-mount imaging of blastoid co-cultured with eSC (EGFP$^+$) without 8-Br-cAMP stained for F-actin and CGB; nuclei stained with Hoechst (blue). Scale bars, 100 µm and 20 µm (magnified). (**E**) Whole-mount imaging of blastoid co-cultured with eSC (EGFP$^+$) stained for OCT4 and CGB (left). Quantification of fused cells with eSC (right); n = 13 blastoids of two independent experiments; ***$P < 0.001$. (**F**) Whole-mount imaging of blastoid co-cultured with eSC (EGFP$^+$) in a collagen-based gel on day 3 stained for VIM and CGB; nuclei stained with Hoechst (blue). Scale bars, 100 µm and 20 µm (magnified). The dashed lines delineate fused cells. (**G**) Whole-mount imaging of blastoid (KuO$^+$) co-cultured with eSC (EGFP$^+$) stained for VIM; nuclei stained with Hoechst (blue). Arrows point out to EGFP$^+$/VIM$^-$ cells. Scale bar, 50 µm.

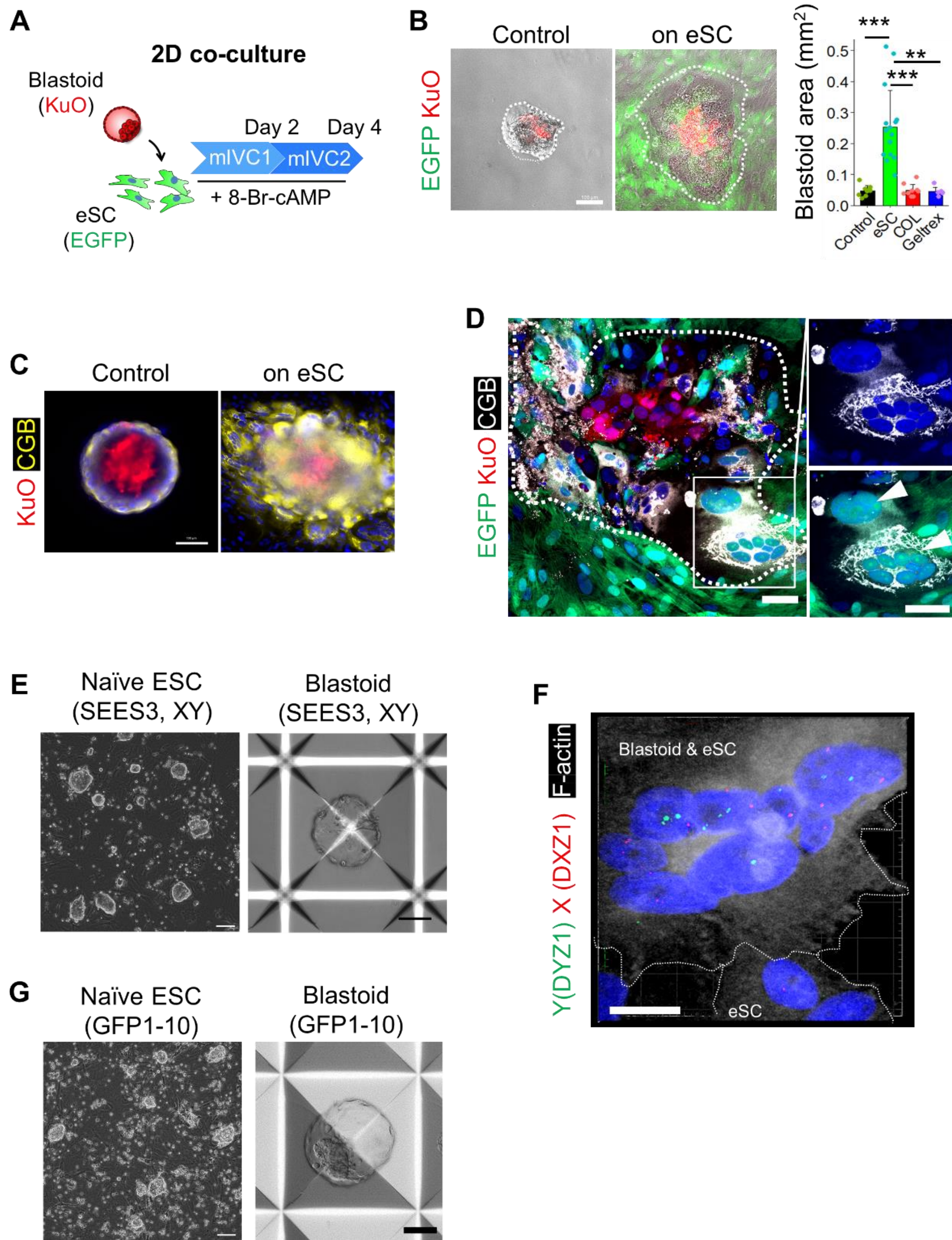

Fig. S8. 2D co-culture of blastoids and eSC. (**A**) Schematic illustration of 2D co-culture experiment. (**B**) Phase contrast and fluorescence images of adhered blastoids (KuO^+) with or without eSC ($EGFP^+$) (left). Scale bar, 100 µm. Quantification of adhered-blastoid area on culture plate (Control), eSC, type I collagen-coated dish (COL), and Geltrex-coated dish (Geltrex) (right); Data shown as mean ± SD; ****P* < 0.001, ***P* < 0.01; n = 9 (Control), 16 (eSC), 10 (COL), and 6 (Geltrex) blastoids. (**C**) Fluorescence images of adhered blastoids

(KuO^+) on culture plate (Control) or eSC (on eSC) stained for CGB; nuclei stained with Hoechst (blue). Scale bar, 100 µm. (**D**) Fluorescence images of adhered blastoid (KuO^+) on eSC ($EGFP^+$) stained for CGB; nuclei stained with Hoechst (blue). Arrowheads indicate CGB^+ cells incorporating $EGFP^+$ eSC nuclei. Scale bars, 50 µm. (**E**) Phase contrast image of naïve ESC (SEES3 line) and bright-field image of SEES3-derived blastoid. Scale bars, 100 µm. (**F**) X (DXZ1) and Y (DYZ1) chromosome detection of multi-nucleated cells in blastoid (SEES3-derived) co-cultured with eSC stained for F-actin. Maximum projection of fluorescence image; nuclei stained with Hoechst (blue). Scale bar, 20 µm. The dashed lines delineate the outlines of the cells based on the cytoplasm stained for F-actin. (**G**) Phase contrast image of naïve ESC and bright-field image of blastoid, both expressing GFP1-10. Scale bars, 100 µm.

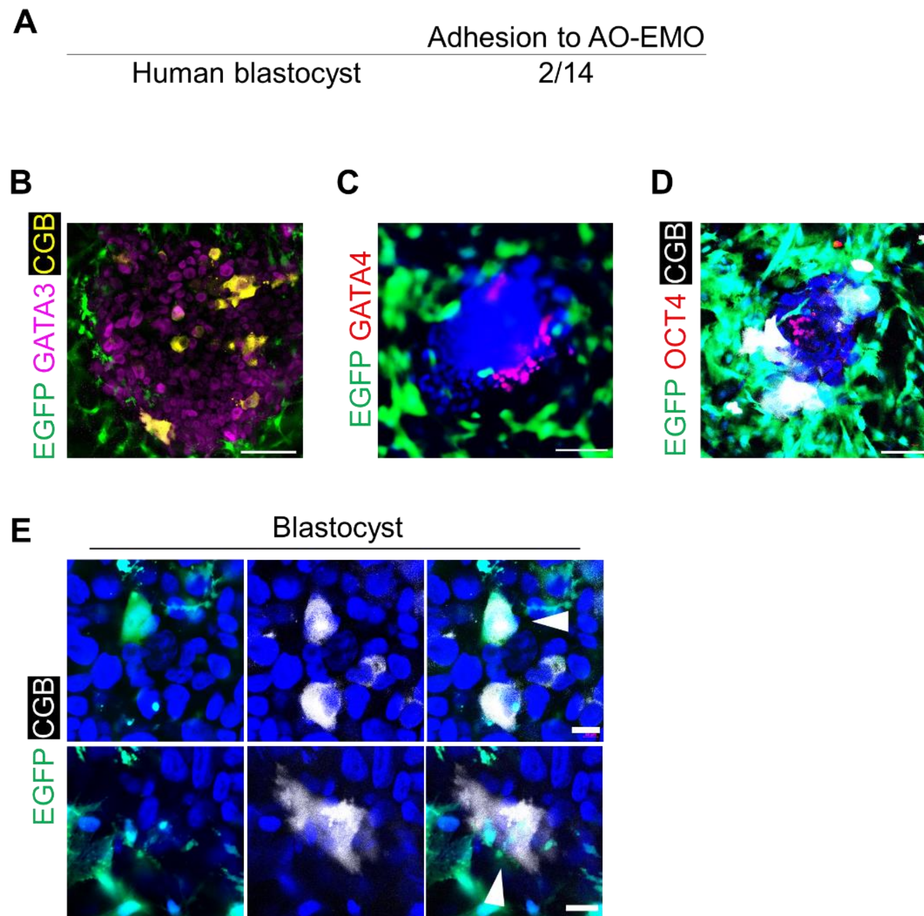

Fig. S9. Culture and analysis of human blastocysts for investigating interaction with endometrial cells. (**A**) Quantification of attached human blastocysts. (**B** to **D**) Whole-mount imaging of human blastocyst co-cultured with eSC (EGFP^{+}) in collagen-based gel on day 3 stained for GATA3, CGB (B), GATA4 (C), and OCT4, CGB (D); nuclei stained with Hoechst (blue). Scale bars, 100 µm. (**E**) Whole-mount imaging of human blastocyst co-cultured with eSC (EGFP^{+}) in collagen-based gel on day 3 stained for CGB; nuclei stained with Hoechst (blue). Arrowheads indicate CGB^{+}/EGFP^{+} fused cells. Scale bars, 20 µm.

Table S1. Antibodies used in this study.

Antibody	Supplier	Cat#
Mouse anti-EpCAM	Cell Signaling	Cat#2929S
Rabbit anti-laminin	Abcam	Cat#ab11575
Rabbit anti-SOX9	Atlas antibodies	Cat#HPA001758
Rabbit anti-PGR	Cell Signaling	Cat#8757S
Rabbit anti-vimentin	Cell Signaling	Cat#5741S
Mouse anti-acetylated α-tubulin	Sigma	Cat#T7451-25UL
Rabbit anti-cleaved caspase 3	Cell Signaling	Cat#9661T
Mouse anti-SDC1 (PE-conjugated)	Miltenyi Biotec	Cat#130-081-301
Rabbit anti-Oct4A	Cell Signaling	Cat#2840S
Mouse anti-CGB	Abcam	Cat#ab9582
Rabbit anti-hCG	Dako	Cat#IS508
Rat anti-GATA4	Thermo Fisher	Cat#14-9980-82
Rabbit anti-NR2F2	Abcam	Cat#ab211776
Rabbit anti-CD31	Abcam	Cat#ab134168
Rabbit anti-Desmoplakin (DSP)	Proteintech	Cat#23518-1-AP
Mouse anti-CD73 (PE-conjugated)	BioLegend	Cat#344004
Mouse anti-CD90 (FITC-conjugated)	eBioscience	Cat#11-0909-42
Goat anti-rabbit IgG (Alexa Fluor 488-conjugated)	Cell Signaling	Cat#4412
Goat anti-mouse IgG (Alexa Fluor 488-conjugated)	Cell Signaling	Cat#4408
Goat anti-rabbit IgG (Alexa Fluor 555-conjugated)	Cell Signaling	Cat#4413
Goat anti-mouse IgG (Alexa Fluor 555-conjugated)	Cell Signaling	Cat#4409
Goat anti-rabbit IgG (Alexa Fluor 647-conjugated)	Cell Signaling	Cat#4409
Goat anti-mouse IgG (Alexa Fluor 647-conjugated)	Cell Signaling	Cat#4409
Rabbit anti-FITC	ThermoFisher	Cat#71-1900
Mouse anti-Biotin	Abcam	Cat#ab201341

Data S1. (separate file)
Oligonucleotides used in this study.

Data S2. (separate file)
RNA-seq sample information and processed data.

Data S3. (separate file)
snRNA-seq sample information and differentially expressed genes (DEGs) list.